Absolute ^{96}Mo$(p, n)^{96m+g}$Tc cross sections and a new branching for the ^{96m}Tc decay

F. Heim,* M. Müller, S. Wilden, and A. Zilges
University of Cologne, Institute for Nuclear Physics, 50937 Köln, Germany

(Received 29 December 2020; revised 13 April 2021; accepted 10 May 2021; published 21 May 2021)

Background: Radionuclides in the Mo-Tc region play an important role in modern medical diagnostics. These applications require a γ-emitting radioisotope that is injected into the patient. Various production methods of those radionuclides have been investigated in the past; among them are (p, x) reactions on natural or enriched molybdenum. Reliable estimations for the produced activity of the radionuclides and radioactive byproducts are required. Therefore, either precise theoretical calculations or a firm experimental database for the nuclear production reactions are needed. In addition, experimental cross-section data of proton-induced reactions on heavy nuclei are very valuable to test nuclear models that enter theoretical calculations of reaction rates relevant for nuclear astrophysics.

Purpose: The present paper reports on experimental cross sections of the ^{96}Mo$(p, n)^{96m+g}$Tc reaction. The contribution of the ground-state population as well as for the population of the metastable state in ^{96}Tc are determined individually. The obtained results are very valuable to test existing models that enter statistical model calculations. In addition, the present work aims at remeasuring the branching ratio of the decay of the metastable state ^{96m}Tc.

Method: Highly enriched ^{96}Mo targets were irradiated with protons at energies between $E_p = 3.9$ MeV and $E_p = 5.4$ MeV, which are slightly above the (p, n) threshold ($E_{th} = 3.8$ MeV). By employing an offline analysis, the γ-ray decay of the reaction product was investigated and reaction cross sections were calculated by means of the activation technique.

Results: Individual reaction cross sections for the production channel of the metastable state σ_m and the ground state σ_{gs} as well as the branching of the ^{96m}Tc $\rightarrow$ ^{96}Tc decay were determined.

Conclusion: The measured cross sections are in good agreement with previously measured cross sections as well as with recent Hauser-Feshbach calculations. The new branching ratio for the direct decay of ^{96m}Tc into ^{96}Mo amounts to $4.1\,^{+0.39}_{-0.34}$ % compared to previously reported 2 ± 0.5%.

DOI: 10.1103/PhysRevC.103.054613

I. INTRODUCTION

In nuclear medicine the use of radionuclides as tracer material plays an important role. Among several others, ^{99m}Tc represents the most frequently used isotope for medical diagnostics [1]. So far, various methods have been developed to produce either ^{99}Mo (which is used as the so-called ^{99}Mo / ^{99m}Tc generator) or ^{99m}Tc directly. One of the most reasonable approaches is the ^{100}Mo$(p, 2n)^{99m}$Tc reaction [2,3]. However, the extraction process of ^{99m}Tc from the produced material is not isotopically selective, i.e., also other technetium isotopes may be extracted as medical injection material. Additionally, the ^{100}Mo target material is not completely enriched but will always contain contaminants from isotopic neighbors, such as ^{94}Mo, ^{95}Mo, ^{96}Mo, ^{97}Mo, and ^{98}Mo. Consequently, (p, xn) reactions on these isotopes will enable the production of further technetium byproducts. To estimate the impact of these contaminations, either precisely measured cross sections for all reaction channels or reliable theoretical predictions are required [4].

In addition, the use of the technetium isotope ^{96g}Tc has been suggested as an alternative for ^{99m}Tc, which might bring several advantages, such as higher γ-ray energies or longer half-lives [5]. This isotope can be produced via the ^{96}Mo$(p, n)^{96g}$Tc reaction. Due to the higher γ-ray energies emitted by ^{96g}Tc compared to ^{99m}Tc, the penetration depth is increased, allowing scans of deep-lying body regions. The detection of the higher-energetic γ rays can be realized by using electron-tracking Compton cameras [6]. Precisely measured cross sections of the ^{96}Mo$(p, n)^{96g,m}$Tc reaction are therefore of direct relevance for the application of this method.

At present, large-scale studies of (p, x) reactions on natural or enriched molybdenum have been conducted and cross sections for the numerous reactions determined [4,7–9]. From the structure of the technetium isotopic chain in the nuclear shell model, one expects that most of the isotopes have rather long-lived isomeric states. When measuring the reaction cross sections via an offline analysis, the explicit branching ratios of the decay of these isomers have a direct impact on the measured cross sections. Hence, precise measurements of these branching ratios are required for all technetium isomers.

Another motivation for the investigation of the ^{96}Mo$(p, n)^{96g,m}$Tc cross section comes from nuclear astrophysics. For the nucleosynthesis of neutron deficient nuclei—the p nuclei—a huge network of photodisintegration reactions is responsible, and is called the γ process [10–12].

*fheim@ikp.uni-koeln.de

Many of the reactions in the γ process involve unstable nuclei for which no experimental cross-section data are available. Hence, reliable theoretical predictions of cross sections are necessary, and are usually obtained using the statistical model [13]. The outcome of these calculations is generally governed by the nuclear physics input. Among the most important nuclear models are the optical-model potentials (OMPs) which describe the effective interaction between an incident particle and the target nucleus (see, e.g., Ref. [14]). Systematic measurements of (p,γ) and (p,n) reactions are required to test the quality of the employed models and to improve their predictive power. The latter reactions are especially useful to study the OMP for protons, since its relative decay width will always be smaller than the neutron width and, hence, is the dominating factor of the calculated values [15].

In this work, cross sections of the (p,n) reaction on ^{96}Mo leading to ^{96g}Tc and ^{96m}Tc at proton beam energies shortly above the threshold will be presented and compared to statistical model calculations. For the first time, the direct population of the metastable state in ^{96}Tc has been studied via offline γ-ray spectroscopy. The experimental cross sections help us to study the underlying nuclear model for the proton OMP that significantly affects calculations. In addition, from the offline decay curve of the produced $^{96m+g}$Tc a new branching ratio of the ^{96m}Tc $\rightarrow$ ^{96}Tc decay was derived.

II. EXPERIMENTAL DETAILS

Six ^{96}Mo targets with an isotopic enrichment of 96 $\pm$ 0.1 % were prepared as self-supporting foils with a thickness of about 1 mg/cm^2. Isotopic contaminants of ^{95}Mo, ^{97}Mo, and ^{98}Mo with each about 1% abundance are the only non-negligible contents within the target material. However, none of these isotopes can eventually contribute to the production of the reaction product of interest, ^{96}Tc, with noteworthy intensity. The thicknesses were determined using Rutherford backscattering spectrometry (RBS), and the energy loss within the target material was estimated using a SRIM [16] simulation and amounted to about 30 to 50 keV, depending on the incident beam energy. Each target was irradiated with proton beam currents of about 400 nA for 5–20 hours. The number of impinging particles was determined by measuring the current on the target, corrected for δ electrons hitting the target chamber. The value of the current was recorded in 200 ms time intervals. Details about the irradiation setup can be found in Ref. [17]. Over the whole irradiation period, the beam current showed very little fluctuations of less than 2%, as can be seen in Fig. 1 which shows the beam intensity as a function of time for the $E_p = 4.8$ MeV irradiation.

After irradiating the samples, they were transported to a dedicated low-background counting setup for activation measurements. The waiting time between the end of bombardment and start of counting was between 50 and 100 minutes. During this time, all short-lived radioactive byproducts had decayed, but it was ensured that the isotopes of interest ^{96g}Tc ($T_{1/2}$ = 4.28 d) and ^{96m}Tc ($T_{1/2} = 51.5$ min) still had significant activity. A reaction scheme that shows the details of the nuclear reaction is given in Fig. 3. In Sec. IV we discuss the obtained γ-ray spectra as well as possible byproducts in more detail.

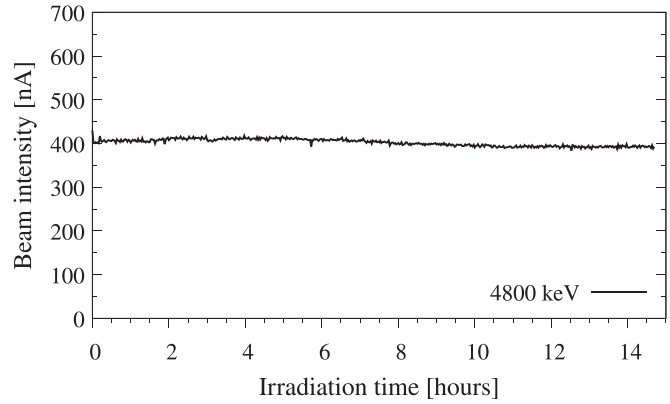

FIG. 1. Beam intensity as a function of irradiation time for the $E_p = 4.8$ MeV activation. The beam was kept at very constant values of about 400 nA. The shown beam current is the effective current on the target corrected for released δ electrons.

The counting setup for the emitted γ-rays consists of two clover-type Ge (high purity) detectors in a very close face-to-face geometry. Each clover detector consists of four individual crystals which all have their own preamplifier and data acquisition. At the typical operating detector-sample distance of 1.3 cm the full-energy peak efficiency of the setup amounts to about 5.3% at a γ-ray energy of $E_\gamma = 1.3$ MeV. The setup is explained in detail in Ref. [18]. During our experiment the detector count rates were not higher than 4 kHz, which corresponds to relative dead times of the data acquisition of lower than $\approx$ 12%. The detectors are located in a low-background room and are shielded with 10 cm of lead in all directions. In addition, 3 mm thick copper plates are mounted on the inside of the lead castle to suppress x-ray background. The overall background count rate of the setup is about 60 Hz.

True coincidence summing effects were calculated using a GEANT4 [19] simulation of the setup. For this, the GEANT4 simulation was run in two modes: First, the complete decay pattern of the radioactive reaction product ^{96}Tc was taken into account, i.e., all γ-ray transitions with their respective intensity are considered. In the second mode only the γ-ray transitions of interest were allowed in the simulation. In both modes the same amount of decaying nuclei was used. Due to the summing effects, the total peak volume of the γ-ray transitions of interest is smaller in the first mode. Figure 2 shows the obtained histograms for both modes ran for the decay of ^{96g}Tc. It can be clearly observed that in mode 1 (complete decay pattern) all γ rays are emitted that are part of the radioactive decay of ^{96g}Tc. The summing effect analysis was performed for ^{96g}Tc and ^{96m}Tc, respectively. Some samples were measured at a much larger distance of 10 cm to the detector, because the produced activity was sufficiently high. At those distances summing effects are almost negligible. At the very short distance of 1.3 cm the coincidence summing has an impact of about 20%.

III. THE ACTIVATION METHOD

The activation technique is a well-established method frequently used for cross-section measurements. This is a

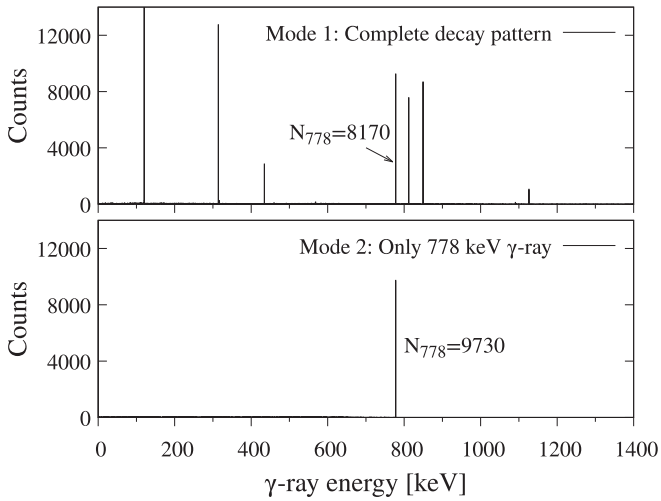

FIG. 2. Summing-effect analysis using a GEANT4 simulation of the detector setup at a sample-detector distance of 1.3 cm. The top panel shows the simulated γ-ray histogram for the decay of ^{96g}Tc including all subsequently emitted γ rays with their respective intensities. The lower panel shows the results of the simulation when only the γ-ray transition with an energy of 778 keV is allowed. Due to the summing effects, the total peak volume is effectively smaller, when the complete decay pattern is taken into account, because the γ rays of interest might be detected coincident with other γ rays, causing the presence of summing peaks at the sum of both of their γ-ray energies. The simulation in each mode included the decay of 10^6 nuclei.

two-step technique where in a first step radioactive isotopes are produced and in a second step the number of produced nuclei are counted. In most cases the counting process is realized by detecting the radioactive decay by the emitted γ rays. See Ref. [20] for a recent review article on the activation technique and its manifold applications.

In a two-member decay chain, where the nucleus X has a long-lived metastable state X^*, which can either decay via internal conversion into the ground state X or via β decay into nucleus Y, three decay chains occur:

$$X \longrightarrow Y, \tag{1}$$

$$X^* \longrightarrow X \longrightarrow Y, \tag{2}$$

$$X^* \longrightarrow Y. \tag{3}$$

Consequently, the total number of produced nuclei Y depends on the individual production cross sections for X and X^*. In the following, we will discuss the individual differential equations that describe the above processes and derive equations to determine the involved cross sections.

A. The differential equations governing the number of produced $^{96m+g}$Tc

During the irradiation the number of ^{96}Tc nuclei produced in their metastable state N_m is given by the differential equation

$$\frac{dN_m}{dt} = P_m(t) - \lambda_m N_m, \tag{4}$$

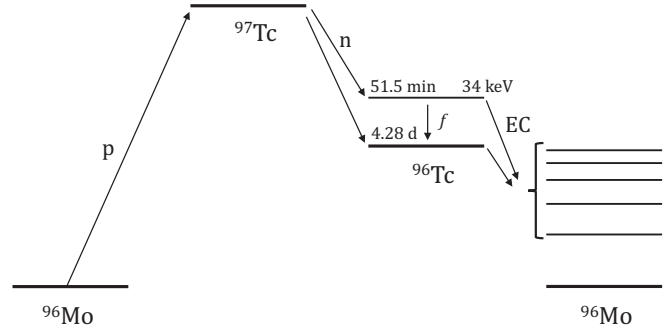

FIG. 3. Schematic illustration of the reaction mechanisms following the proton capture on ^{96}Mo. The metastable state in ^{96}Tc can either decay via internal conversion into its ground state with a branching ratio of f or it can decay via electron capture directly into ^{96}Mo with a branching of $1-f$.

where $P_m(t) = \sigma_m N_T \Phi$ denotes the production rate with σ_m the reaction cross section, N_T the number of target nuclei and Φ the particle flux. In the following we will assume a constant production rate, i.e., $P(t) = P$. In Sec. II this assumption has been justified for the present experiment. Generally, the activation technique can also be applied if the particle beam is not constant since it is recorded in time steps of 200 ms and an iterative algorithm can be employed to account for possible fluctuations. The decay constant is given by $\lambda_m = \ln(2)/T^m_{1/2}$. The solution of this differential equation, and hence the number of ^{96m}Tc nuclei as a function of time after the end of irradiation, is

$$N_m(t) = \frac{P_m(1 - e^{-\lambda_m t_A})e^{-\lambda_m t}}{\lambda_m}, \tag{5}$$

where $t = 0$ denotes the end of irradiation and t_A the total activation time. On the other side, the number of ^{96}Tc nuclei in their ground state N_g can additionally increase by decays of the metastable state:

$$\frac{dN_g}{dt} = P_g(t) - \lambda_g N_g + f\lambda_m N_m. \tag{6}$$

Here, $P_g(t)$ is the production rate of the ground state, λ_g the decay constant of ^{96g}Tc, and f denotes the branching ratio of the decay ^{96m}Tc $\rightarrow$ ^{96g}Tc. Analogously to the situation above, the number of ^{96g}Tc nuclei as a function of time after the end of irradiation is given by

$$N_g(t) = \frac{1}{\lambda_g}\left(P_g + f\frac{\lambda_m}{\lambda_m - \lambda_g}P_m\right)(1 - e^{-\lambda_g t_A})e^{-\lambda_g t} - \frac{f}{\lambda_m - \lambda_g}P_m(1 - e^{-\lambda_m t_A})e^{-\lambda_m t}. \tag{7}$$

B. The production cross section of the metastable state

The metastable state in ^{96}Tc at an excitation energy of 34 keV has a half-life of 51.5 minutes (see Fig. 3). Its decay into the ground state barely leaves any observable γ-ray fingerprint since the respective γ ray has a very low energy and very low intensity of 0.0259%. However, with a reported

branching of 2%, ^{96m}Tc can decay via electron capture (EC) into ^{96}Mo and subsequently emit several γ-ray transitions that can be unambiguously assigned to the decay of this isomer. Hence, by employing Eq. (5) and the known activation formula (see, e.g., Ref. [20]), the production cross section for the metastable state can be calculated via

$$\sigma_m = \frac{\lambda_m N_\gamma e^{\lambda_m t_W}}{\Phi I_\gamma \epsilon(E_\gamma)\tau N_T (1 - e^{-\lambda_m t_A})(1 - e^{-\lambda_m t_C})}, \tag{8}$$

where N_γ denotes the peak volume of the transition of interest, I_γ the respective intensity, ϵ the full-energy peak efficiency at the respective γ-ray energy of interest E_γ, t_W the waiting time, τ the dead-time correction factor, and t_C the counting time.

C. The effective ground-state production cross section

If one waits long enough between the end of irradiation and begin of the counting to ensure that nearly all nuclei in the metastable state have decayed, Eq. (7) simplifies to

$$N_g(t) = \frac{1}{\lambda_g}\left(P_g + f\frac{\lambda_m}{\lambda_m - \lambda_g}P_m\right)(1 - e^{-\lambda_g t_A})e^{-\lambda_g t}. \tag{9}$$

By applying the known activation formula, the effective total cross section is obtained from

$$\begin{aligned}\sigma_{\text{eff}} &= \sigma_g + f\frac{\lambda_m}{\lambda_m - \lambda_g}\sigma_m \\ &= \frac{\lambda_g N_\gamma e^{\lambda_g t_W}}{\Phi I_\gamma \epsilon(E_\gamma)\tau N_T (1 - e^{-\lambda_g t_A})(1 - e^{-\lambda_g t_C})},\end{aligned} \tag{10}$$

where all parameters have the same meaning as in Eq. (8). Note that different γ-ray transitions have been used to determine the cross sections σ_m and σ_{eff}. See Table I for details of the observed γ-ray transitions and their intensities.

D. Calculating the ^{96m}Tc → ^{96g}Tc decay branching

In contrast to the case described in Sec. III C we can also give an expression for the number of ^{96g}Tc nuclei at the end of irradiation:

$$\begin{aligned}N_g(0) = &\frac{1}{\lambda_g}\left(P_g + f\frac{\lambda_m}{\lambda_m - \lambda_g}P_m\right)(1 - e^{-\lambda_g t_A}) \\ &- \frac{f}{\lambda_m - \lambda_g}P_m(1 - e^{-\lambda_m t_A}).\end{aligned} \tag{11}$$

By employing the expression after the first equal sign in Eq. (10), regrouping in terms of the production rates P_{eff} and P_g, and solving for $\sigma_g = \frac{P_g}{N_T \Phi}$, we obtain for the production cross section of the ground state of ^{96}Tc

$$\begin{aligned}\sigma_g = &\frac{N_g(0)\lambda_m}{N_T \Phi(1 - e^{-\lambda_m t_A})} \\ &+ \sigma_{\text{eff}}\left(1 - \frac{\lambda_m}{\lambda_g}\frac{(1 - e^{-\lambda_g t_A})}{(1 - e^{-\lambda_m t_A})}\right).\end{aligned} \tag{12}$$

Again, using the first equivalence in Eq. (10), the branching ratio f that describes how many ^{96m}Tc nuclei decay into the ground state relative to the total number of decays is given by

$$f = \frac{(\sigma_{\text{eff}} - \sigma_g)}{\sigma_m}\frac{\lambda_m - \lambda_g}{\lambda_m}. \tag{13}$$

However, the calculated cross section σ_m depends on the γ-ray intensities [see Eq. (8)] for which the reported values are normalized to the total branching of 2% for the EC decay. This branching ratio shall be remeasured within this work; therefore, we introduce the expression

$$\tilde{\sigma}_m = \sigma_m\frac{(1 - f)}{(1 - \tilde{f})} = \sigma_m\frac{0.02}{(1 - \tilde{f})}, \tag{14}$$

where σ_m denotes the calculated cross section using the reported branching ratio for the EC decay of $(1 - f) = 2\%$. If the true branching, denoted as $\tilde{f}$, differs from f, the γ-ray intensities I_γ need to be renormalized to the true branching, and the true cross section $\tilde{\sigma}_m$ will change as well according to this equation. We substitute σ_m and f with $\tilde{\sigma}_m$ and $\tilde{f}$ in Eq. (13) and define the term on the right-hand side as c:

$$\tilde{f}\tilde{\sigma}_m = (\sigma_{\text{eff}} - \sigma_g)\frac{\lambda_m - \lambda_g}{\lambda_m} =: c. \tag{15}$$

Using Eq. (14) delivers the expression for the true branching ratio $\tilde{f}$:

$$\tilde{f} = \frac{c}{\sigma_m(1 - f) + c}. \tag{16}$$

TABLE I. γ-ray transitions used for the activation analysis of the produced ^{96m}Tc and ^{96g}Tc nuclei. For each transition the absolute intensities reported in Ref. [21] are given.

Isotope	Daughter	f (%)	Half-life	E_γ	I_γ (%)
^{96m}Tc	^{96g}Tc	98.0(5)	51.5(10) min	34.20(5)[a]	0.0259(4)
^{96m}Tc	^{96}Mo	2.0(5)	51.5(10) min	966.4(2)	0.045(12)
				968.5(2)	0.081(21)
				1237.8(2)	0.013(3)
				1815.6(5)	0.039(10)
				1846.2(2)	0.0045(13)
				1957.1(5)	0.0094(25)
^{96g}Tc	^{96}Mo	100	4.28(7) d	314.27(5)	2.43(24)
				316.50(6)	1.4(2)
				434.71(5)	0.75(5)
				460.04(7)	0.43(4)
				481.0(4)	0.08(3)
				535.78(8)	0.41(4)
				568.88(7)	0.92(6)
				778.22(4)	99.76(5)
				812.54(4)	82(3)
				849.86(4)	98(4)
				885.40(20)	0.10(4)
				1091.30(4)	1.10(8)
				1126.85(6)	15.2(12)
				1200.17(8)	0.37(3)
				1441.14(10)	0.054(6)
				1497.72(10)	0.093(7)

[a]This transition has not been observed.

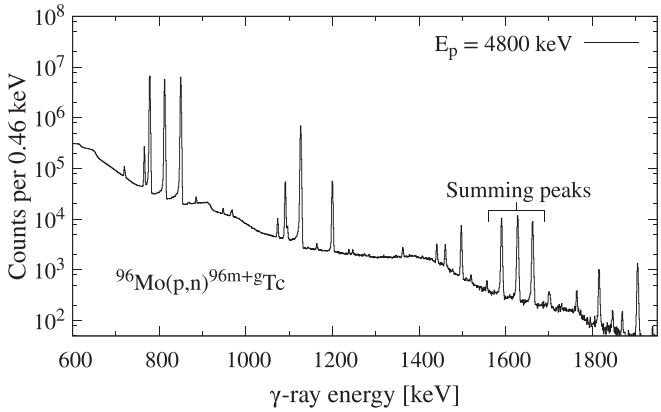

FIG. 4. Typical γ-ray spectrum from a 6 hour offline counting after the ^{96}Mo$(p,n)^{96}$Tc reaction using 4800 keV protons. All visible peaks originate from the EC decay of ^{96}Tc. The three smaller peaks at around 1600 keV are the result of true coincidence summing effects of the three peaks at around 800 keV. The summing effects have been estimated using a GEANT4 [19] simulation (see Sec. II for details).

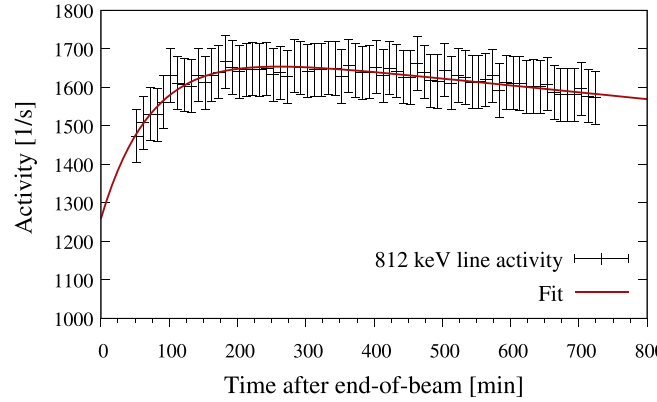

FIG. 5. Measured absolute activity of the 812 keV line from the decay of ^{96g}Tc as a function of time after the end of bombardment. The fit function given in Eq. (17) is employed to derive the number of ^{96g}Tc nuclei at the end of bombardment.

IV. RESULTS AND ANALYSIS

A typical γ-ray spectrum from the offline counting is presented in Fig. 4. Due to isotopic contaminants within the target material the presence of other radioactive species within the samples is possible. The only other reaction channel that would lead to the co-production of ^{96}Tc apart from our reaction of interest is the ^{95}Mo$(p,\gamma)^{96}$Tc reaction (see Sec. II for target details). However, the expected cross sections for this reaction in the measured energy region are about two orders of magnitude smaller than those for the ^{96}Mo$(p,n)^{96}$Tc reaction. In combination with the lower atomic abundance in the target material by additional two orders of magnitude, the total impact of this reaction channel can be neglected.

Essentially, for the other Mo isotopes that are present in the samples, only the (p,n) reactions possess cross sections of considerable magnitude to contribute to the production of undesired byproducts. In detail, these are ^{95}Mo$(p,n)^{95}$Tc, ^{97}Mo$(p,n)^{97}$Tc, and ^{98}Mo$(p,n)^{98}$Tc. For ^{97}Tc and ^{98}Tc, however, the respective half-lives are in the order of million years, which would lead to very low produced activities. In fact, no γ-ray fingerprint for either of these isotopes was found during the γ-ray analysis. For ^{95}Tc the half-life amounts to 20.0 hours and the strongest γ-ray transitions emitted during its decay are at 766, 948, and 1074 keV. The strongest transition at $E_\gamma = 766$ keV was found to have a total intensity that is lower by about two orders of magnitude compared to the strongest transition in ^{96}Tc at $E_\gamma = 778$ keV. Moreover, the peaks of interest (see Table I) are well resolved and can be unambiguously assigned to the reaction product of interest, ^{96}Tc.

Following the above discussion, we conclude that all strong, visible peaks can be assigned to the reaction products $^{96m+g}$Tc and no contamination from other sources has been found. For the electron-capture decay of ^{96m}Tc six γ-ray transitions have been observed (see Table I). The half-life of this isotope is only about 51 minutes, which means that a considerable amount of produced nuclei have decayed between the end of irradiation and begin of γ-ray counting. Nevertheless, due to the large number of reaction products the peak volumes of the respective γ-ray transitions had sufficient intensity to provide statistical uncertainties of less than 5%.

The number of ^{96g}Tc nuclei increases after the end of irradiation proportional to $(1 - e^{-\lambda_m t})$. This increase is driven by the progressive production of ^{96g}Tc due to the decay of ^{96m}Tc nuclei and can be particularly observed in the case of the 812 keV line, since this can only stem from the ^{96g}Tc decay. Hence, we chose to study the absolute activity of this line as a function of time, which is described by the expression

$$N_{812}(t) = N_g(0)e^{-\lambda_g t} + fN_m(0)\frac{\lambda_m}{\lambda_m - \lambda_g}(e^{-\lambda_g t} - e^{-\lambda_m t}) \tag{17}$$

to deduce the number of ^{96}Tc nuclei in the ground state at the end of bombardment. The activity curve was determined for each of the six beam energies. Figure 5 shows as an example the decay curve after the $E_p = 3900$ keV bombardment along with the corresponding fit function, where $N_g(0)$ and $N_m(0)$ are the fit parameters.

A. Calculation of the absolute intensity of the 812 keV transition

From the number of γ-rays N_γ counted during the offline analysis, the absolute activity is given by

$$A_{812} = \frac{N_\gamma}{\epsilon(812)\tau I_\gamma t}, \tag{18}$$

where $\epsilon(812)$ denotes the detection efficiency at 812 keV, τ the dead-time correction factor of the detector, I_γ the γ-line intensity, and t the measuring time, which was typically 10 minutes for each counting interval. The uncertainty of the measured activity of the 812 keV line depicted in Fig. 5 is mainly governed by the large systematic uncertainty of the intensity, which amounts to $(82 \pm 3)\%$ [21]. All other parameters have only very small contribution to the total uncertainty. However, the fit results are very sensitive to the absolute number of decays and, consequently, the calculated branching ratio $\tilde{f}$ for the ^{96m}Tc $\rightarrow$ ^{96}Tc decay depends strongly on the

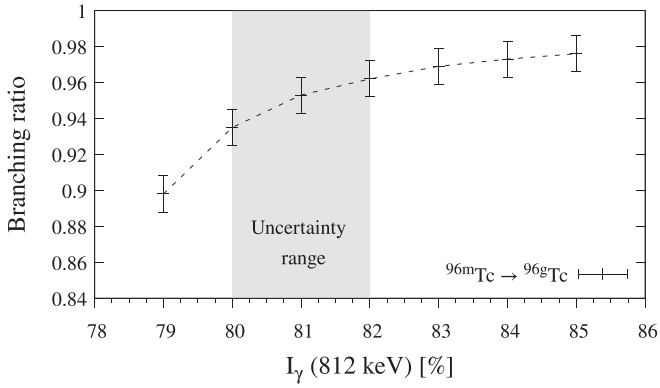

FIG. 6. Branching ratio f that describes how many ^{96m}Tc nuclei decay into the ^{96}Tc ground state relative to the total amount of ^{96m}Tc decays for different γ-ray intensities of the 812 keV line. The formerly reported intensity of (82 ± 3)% [21] has been revised in this work. The new measured value amounts to (81 ± 1)%. Consequently, the uncertainty of the branching ratio f is governed by this uncertainty region (shown as the grey shaded region).

γ-ray intensity. Figure 6 shows the calculated branching ratio for various assumed intensities of the 812 keV line between 79% and 85%. It should be clear that I_γ has to be pinned down before a reliable value for $\bar{f}$ can be given.

For this reason, the γ-ray intensity of the 812 keV line was remeasured by using γ-ray spectra recorded about 15 hours after the end of bombardment and was normalized to the peak volume of the 779 keV line. These long-term counting measurements were available for two beam energies and the intensity of the 812 keV transition was determined independently for both measurements. The results shown in Table II hint to a lower branching ratio of (81.0 ± 1) %, where the uncertainty is governed by the true coincidence summing estimations using GEANT4 [19].

B. Cross sections and branching ratio

Table III lists the resulting cross sections for each beam energy calculated by means of Eqs. (8), (10), and (12) as well as the calculated true branching ratios for the ^{96m}Tc → ^{96}Tc decay. This branching ratio f describes the number of ^{96m}Tc nuclei that decay into the ground state of ^{96}Tc compared to the total number of decays. The final branching ratio was calculated as the weighted mean of all measurements, and yields a value of

$$\bar{f} = 95.9\,^{+0.34}_{-0.39}\,\%,$$

where the error of each individual value is given by the range of values that lies within the corresponding uncertainty range

TABLE II. The absolute intensity of the 812 keV line I_γ(812) was measured using two independent countings. The new intensity of 81 ± 1% is lower than the previously used value of 82 ± 3% [21].

Counting No. 1	Counting No. 2	Mean	Literature
81.0(1) %	81.0(1) %	81.0(1) %	82(3) %

TABLE III. Measured cross sections σ_m, σ_g, and σ_{tot} as well as the derived branching ratio for the ^{96m}Tc → ^{96}Tc decay for each individual center-of-mass energy of the ^{96}Mo$(p,n)^{96}$Tc reaction.

$E_{c.m.}$ (MeV)	σ_m (mb)	σ_g (mb)	σ_{tot} (mb)	f (%)
3.836(22)	1.82(20)	0.65(35)	2.47(40)	$96.7\,^{+0.5}_{-0.8}$
4.133(22)	7.03(78)	4.9(13)	11.9(15)	$95.8\,^{+1.1}_{-1.0}$
4.428(22)	15.9(17)	6.0(14)	21.9(22)	$96.1\,^{+0.7}_{-0.6}$
4.730(22)	18.6(20)	15.5(40)	34.1(45)	$95.4\,^{+0.9}_{-1.8}$
5.024(22)	28.1(35)	21.9(33)	50.0(48)	$95.4\,^{+0.5}_{-0.6}$
5.323(22)	69.4(75)	41(10)	110(13)	$96.2\,^{+0.9}_{-1.7}$

of the intensity of the 812 keV transition (see Fig. 6). Note that all γ-ray intensities that were used to calculate σ_m by means of Eq. (8) were renormalized to the new branching ratio. The direct impact of the new branching for nuclear medicine applications is expected to be rather small as it triggers only a small relative change of the number of produced ^{96g}Tc nuclei. However, the activity of the electron-capture decay of ^{96m}Tc increases by a factor of about 2 when taking the new branching ratio into account. In general, a systematic remeasurement of branching ratios of metastable states in the Tc isotopes is mandatory and possible by means of the activation method as presented in this work.

Figures 7 and 8 show the newly determined cross-section values for the ^{96}Mo$(p,n)^{96m}$Tc as well as for the ^{96}Mo$(p,n)^{96m+g}$Tc reaction along with previously measured data from Refs. [22,23]. In addition, the results of statistical model calculations using the Hauser-Feshbach code TALYS in version 1.95 [13] are illustrated.

The TALYS calculations were performed with default settings, that is, the optical model potential parametrization from Koning and Delaroche [14] for neutrons and protons, the Brink-Axel Lorentzian for the dipole strength function [24,25], and the constant temperature Fermi gas model introduced by Gilbert and Cameron for the nuclear level density [26]. As explained in the Introduction, (p,n) reactions are predominantly sensitive to the proton OMP. Since its publication,

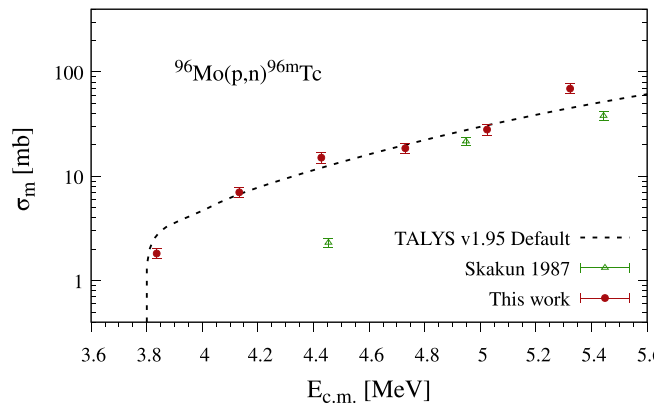

FIG. 7. Measured cross sections of the ^{96}Mo$(p,n)^{96m}$Tc reaction as a function of center-of-mass energy along with statistical model calculations using the TALYS code version 1.95 with default parameters as well as with previously reported results from Ref. [22].

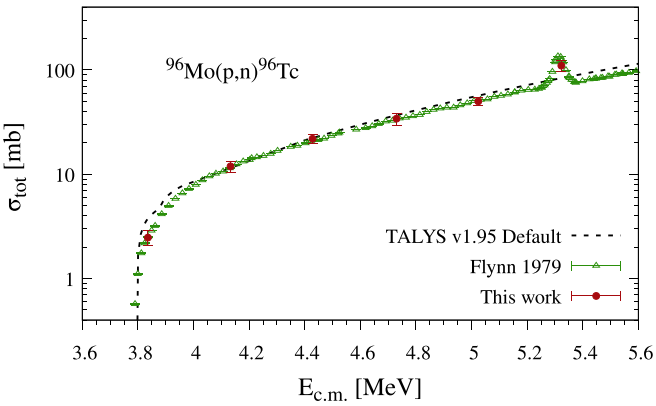

FIG. 8. The same as Fig. 7 but for the total ^{96}Mo$(p,n)^{96}$Tc cross section. Also, experimental results from Flynn *et al.* are shown [23].

remarkable success has been observed for the Koning and Delaroche model in describing almost all (p,n) cross sections at sub-Coulomb energies; see, e.g., Refs. [27–29].

For the first time, cross sections for the direct population of the metastable state ^{96m}Tc have been measured by using offline γ-ray counting. The results are compared to previously measured data. However, the reported values from Ref. [22] seem to scatter in the region of interest and show surprisingly small uncertainties. Hence, a meaningful comparison is not possible. In contrast, the calculated TALYS cross section seem to be in good agreement with the values derived in this work.

The total cross sections of the ^{96}Mo$(p,n)^{96}$Tc reactions derived in this work are in very good agreement with previous studies from Flynn *et al.* reported in Ref. [23]. The TALYS calculations are also in good agreement as they lie within the range of uncertainties for all data points except for the lowest energy of 3.9 MeV and the energy region around 5.3 MeV. The former one might be explained by the fact that it lies just above the (p,n) threshold. That means the (p,n) cross section might be sensitive to not only the OMPs but also to the γ-ray transmission coefficients of the competing (p,γ) channel. Nevertheless, within the uncertainty in beam energy the lowest data point barely touches the TALYS predictions.

In the region around $E_p = 5.3$ MeV a resonance for the (p,n) cross section was found in Ref. [23], which has been nicely reproduced within the present experiment. However, this resonant behavior of the cross section in this region seems to be not reproducible by theory.

The overall agreement between the statistical model calculations and our experimental data confirms the reliability and quality of the employed OMP employed in these calculations. In particular, the deviations between experiment and theory are much smaller than required for astrophysical applications, where reaction rates are often uncertain by a factor of 2 [11,30]. Finally, well-constrained OMPs for protons and neutrons help to diminish the uncertainties in calculations which are also affected by other uncertain parameters, such as γ-ray transmission coefficients reactions.

V. SUMMARY AND CONCLUSION

In this work, we reported on the production cross sections of the ^{96}Mo$(p,n)^{96m+g+tot}$Tc reaction. The careful disentanglement of the different production channels allowed us to derive the branching ratio for the direct decay via electron capture of ^{96m}Tc. For that purpose, a novel approach was presented which is based on the solution of the differential equations that describe the decay behavior of the produced ^{96g}Tc and ^{96m}Tc nuclei. It was shown that the branching for the direct decay ^{96m}Tc via electron capture amounts to $4.1\,^{+0.39}_{-0.34}$ % and hence is two times higher than previously assumed. Additionally, the absolute γ-ray intensity of the prominent 812 keV line that appears in the decay of ^{96g}Tc was remeasured. The derived cross sections have been compared to previously reported results and also to theoretical calculations using the Hauser-Feshbach code TALYS v1.95. The overall agreement is very convincing. Hence, the ^{96}Mo$(p,n)^{96}$Tc reaction can be included into the set of reliably measured monitor reactions. This allows reliable estimation of the produced dose of ^{96g}Tc within the cyclotron production of medical radioisotopes. A systematic study of the decay behavior of the technetium isotopes is advisable, and more precise measurements of γ-ray intensities and branching ratios would help to minimize the uncertainties of cross-section measurements. Measuring (p,n) cross sections on heavy nuclei is very valuable as it helps to test nuclear physics input for statistical model calculations. These calculations are used to a great extent to understand the nucleosynthesis of the elements in nuclear astrophysics.

ACKNOWLEDGMENTS

We gratefully thank H. W. Becker and V. Foteinou of the Ruhr-Universität Bochum for the assistance during the RBS measurements. This project has been supported by the Deutsche Forschungsgemeinschaft under the contract ZI 510/9-1.

[1] National Academies of Sciences, Engineering, and Medicine; Division on Earth and Life Studies; Nuclear and Radiation Studies Board, Molybdenum-99/Technetium-99m in Nuclear Medicine, in *Opportunities and Approaches for Supplying Molybdenum-99 and Associated Medical Isotopes to Global Markets: Proceedings of a Symposium*, Washington, DC, 7 February 2018 (National Academies Press, Washington, 2018), available from https://www.ncbi.nlm.nih.gov/books/NBK487238/.

[2] S. Manenti, U. Holzwarth, M. Loriggiola, L. Gini, J. Esposito, F. Groppi, and F. Simonelli, Appl. Radiat. Isot. **94**, 344 (2014).

[3] S. M. Qaim, S. Sudár, B. Scholten, A. J. Koning, and H. H. Coenen, Appl. Radiat. Isot. **85**, 101 (2014).

[4] E. Lamere *et al.*, Phys. Rev. C **100**, 034614 (2019).

[5] G. H. Hovhannisyan, A. S. Danagulyan, and T. M. Bakhsyan, Phys. Atom. Nuclei **82**, 1 (2019).

[6] T. Mizumoto *et al.*, J. Instrum. **10**, C01053 (2015).

[7] J. Červenák and O. Lebeda, Nucl. Instrum. Methods B **380**, 32 (2016).
[8] O. Lebeda and M. Pruszyński, Appl. Radiat. Isot. **68**, 2355 (2010).
[9] F. Tárkányi, F. Ditrói, A. Hermanne, S. Takács, and A. V. Ignatyuk, Nucl. Instrum. Methods B **280**, 45 (2012).
[10] M. Arnould and S. Goriely, Phys. Rep. **384**, 1 (2003).
[11] T. Rauscher, N. Dauphas, I. Dillmann, C. Fröhlich, Z. Fülöp, and G. Gyürky, Rep. Prog. Phys. **76**, 066201 (2013).
[12] M. Pignatari, K. Göbel, R. Reifarth, and C. Travaglio, Int. J. Mod. Phys. E **25**, 04 (2016).
[13] A. Koning and D. Rochman, Nucl. Data Sheets **113**, 2841 (2012).
[14] A. J. Koning and J. P. Delaroche, Nucl. Phys. A **713**, 231 (2003).
[15] T. Rauscher, Int. J. Mod. Phys. E **20**, 1071 (2011).
[16] J. Ziegler, J. Biersack, and M. Ziegler, SRIM - The Stopping and Range of Ions in Matter, http://www.srim.org.
[17] F. Heim, J. Mayer, M. Müller, P. Scholz, M. Weinert, and A. Zilges, Nucl. Instrum. Methods A **966**, 163854 (2020).
[18] P. Scholz, A. Endres, A. Hennig, L. Netterdon, H. W. Becker, J. Endres, J. Mayer, U. Giesen, D. Rogalla, F. Schluter, S. G. Pickstone, K. O. Zell, and A. Zilges, Phys. Rev. C **90**, 065807 (2014).
[19] N. Agostinelli *et al.*, Nucl. Instrum. Methods A **506**, 250 (2003).
[20] G. Gyürky, Z. Fülöp, F. Käppeler, G. G. Kiss, and A. Wallner, Eur. Phys. J. A **55**, 41 (2019).
[21] D. Abriola and A. A. Sonzogni, Nucl. Data Sheets **109**, 2501 (2008).
[22] E. A. Skakun, V. G. Batij, Yu. N. Rakivnenko and O. A. Rastrepin, Yad. Fiz. **46**, 28 (1987).
[23] D. S. Flynn, R. L. Hershberger, and F. Gabbard, Phys. Rev. C **20**, 1700 (1979).
[24] D. M. Brink, Nucl. Phys. **4**, 215 (1957).
[25] P. Axel, Phys. Rev. **126**, 671 (1962).
[26] A. Gilbert and A. G. W. Cameron, Can. J. Phys. **43**, 1446 (1965).
[27] I. Gheorghe *et al.*, Nucl. Data Sheets **119**, 245 (2014).
[28] V. Foteinou, S. Harissopulos, M. Axiotis, A. Lagoyannis, G. Provatas, A. Spyrou, G. Perdikakis, C. Zarkadas, and P. Demetriou, Phys. Rev. C **97**, 035806 (2018).
[29] F. Heim, P. Scholz, J. Mayer, M. Müller, and A. Zilges, Phys. Rev. C **101**, 035807 (2020).
[30] W. Rapp, J. Görres, and M. Wiescher, Astrophys. J. **653**, 474 (2006).